

Network Coding Applications for 5G Millimeter-Wave Communications

Murali Narasimha

Hossein Bagheri

Motorola Mobility Limited

ABSTRACT

The millimeter-wave bands have been attracting significant interest as a means to achieve major improvements in data rates and network efficiencies. One significant limitation for use of the millimeter-wave bands for cellular communication is that the communication suffers from much higher path-loss compared to the microwave bands. Millimeter-wave links have also been shown to change rapidly, causing links between devices and access points to switch among line-of-sight, non-line-of-sight and outage states. We propose using Random Linear Network Coding to overcome the unreliability of individual communication links in such millimeter-wave systems. Our system consists of devices transmitting and receiving network-coded packets through several access points. For downlink communication, network-coded packets are transmitted to a device via multiple access points. For uplink communication, the access points perform network coding of packets of several devices, and then send the network-coded packets to the core network. We compare our approach against a naive approach in which non-network coded packets are transmitted via multiple access points (“Forwarding” approach). We find that the network coding approach significantly outperforms the forwarding approach. In particular, network coding greatly improves the efficiency of the air-interface transmissions and the efficiency of the backhaul transmissions for the downlink and uplink communication, respectively.

1. INTRODUCTION

The mobile communications industry is embarking on a wide-ranging effort to define and build the next generation of wireless systems referred to as 5G. This is driven by large increases in mobile communications usage and expected future growth that is staggering [1],[2]. 5G networks will be expected to deliver as much as 1000 times the data rate of current networks [3], [4].

As part of the 5G initiatives, there is enormous interest in millimeter-wave (MmWave) bands between 30

GHz and 300 GHz [4]-[8], where the available bandwidths are much larger than today’s cellular bands. While millimeter-wave has historically been used for backhaul links and satellite communications, it has not been considered suitable for cellular communications due to the much higher path-loss that mmWave signals experience. In order to overcome the path-loss, it is necessary to use antenna arrays and perform beam-forming [6]. Advances in RF and semiconductor technologies have made the use of mmWave bands more suitable for cellular communications [9]. Specifically, such advances have made it possible to have antenna arrays in areas small enough that they can be practically accommodated inside mobile devices. Such beam-forming is considered an essential enabling technology for millimeter-wave communication.

One distinctive characteristic of mmWave communication compared to microwave is the highly directional nature of the signal path [7], [11]. The beam-formed communication makes the communication links much more directionally sensitive. Obstructions can easily block the communication path; small changes in orientation or small movements may cause “*deafness*” (due to the transmitter and receiver antennas not being correctly pointed at each other) [12]. Events that cause such blocking and deafness are highly unpredictable (mobility, small movements by user, temporary vehicular and other obstructions in the environment, etc.). This makes it necessary to have redundant access points such that in the event of a loss of communication to an access point, the device can quickly switch to a different access point [11]. However, switching to different access points can result in interruptions in communication, with the overall impact of the interruptions dependent on the frequency of the switching and the time the device takes to establish an alternate communication link.

Another distinctive characteristic is that the Doppler spread at mmWave frequencies is much higher for a

given speed, compared to microwave frequencies. This leads to much smaller channel coherence times compared to microwave (for example, at 30 km/h the coherence times for 3 GHz and 30 GHz are 12 ms and 1.2 ms respectively), suggesting that the channel can change very rapidly. Scheduling in such an environment is likely to require very frequent feedback, which tends to consume a lot of resources and energy. Moreover, if the feedback communication occurs in the mmWave band, it is subject to the same link breakage constraints mentioned above.

Relying on the redundancy of access points, we consider an architecture in which a device maintains communication links to a number of access points. Data can be transmitted from any of the access points to the device and from the device to any of the access points. We use network-coding techniques for data transmission on both the downlink and the uplink. The general idea is that such an approach is less dependent on frequent feedback, and the device continues to receive (or transmit) the same data stream through some sub-set of the access points even as connections to individual access points are interrupted.

The paper is organized as follows. Section 2 summarizes some of the related work in the area of millimeter wave communications and network coding. Section 3 introduces the system model and describes our use of Random Linear Network Coding. We describe metrics that enable comparison of the network coding based transmissions to conventional transmissions schemes. We also derive bounds and estimates for the comparison metrics. Section 4 provides results of a Monte-Carlo system simulation performed to understand the benefits of network coding in a millimeter-wave deployment with access points deployed along a street. Section 5 has our concluding remarks and observations on possible future work.

2. RELATED WORK

Millimeter-wave for cellular networks has received a lot of attention recently [4]-[10]. The issues related to directionality of transmissions and the need for frequent handovers have been studied in [12]. Deployments of Millimeter-wave access points for typical scenarios (street-side, stadium, etc.) are considered and it is shown that, due to the directionality and blocking properties, handovers occur much more frequently than microwave networks.

Current cellular networks generally rely on the principle of having a single serving access point. However,

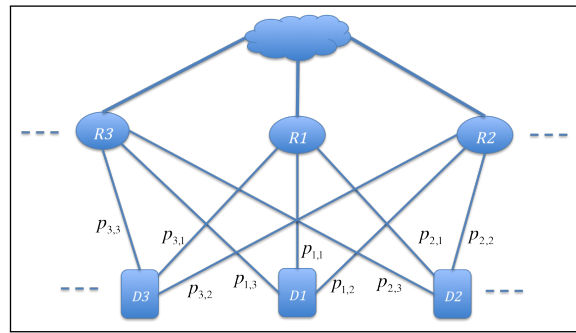


Figure 1: Block diagram of a network consisting of multiple Relay Nodes and multiple devices

some enhancements, which involve devices maintaining simultaneous links to different access points, have been standardized. For example, Carrier Aggregation in LTE [13] allows for a device to be connected to and communicate with multiple spatially separated nodes (Coordinated Multi-point Transmission). Another example is Dual Connectivity in LTE [13], which allows for concurrent communication with different (spatially separated) access points, each independently scheduling packets for the device.

Network Coding was first proposed in [14] as a methodology for improving throughput for multicast applications by transmitting “combinations” of packets. There have been some studies of applications of network coding to wireless communications [15]-[17]. To the best of our knowledge, there has not been any prior work on investigating the applicability of network coding to millimeter wave cellular networks.

3. SYSTEM MODEL

We consider a radio network comprising multiple relay nodes $R1, R2, \dots, RN$ serving one or more devices $D1, D2, \dots, DN$ as shown in Figure 1. Each device maintains mmWave communication links to a set of relay nodes and data is concurrently transmitted to and received from the device through the set of relay nodes. The relay nodes are connected to the network through backhaul links, which could be wired, or wireless. Thus, the physical realization of the relay nodes described here could be in the form of small cells, wireless relays or remote radio heads.

Links between the devices and relay nodes are modeled as packet erasure channels; $p_{i,j}$ represents the packet erasure probability of the millimeter-wave link between device Di and relay node Rj . The packet erasure probabilities are time varying and their modeling is described further below.

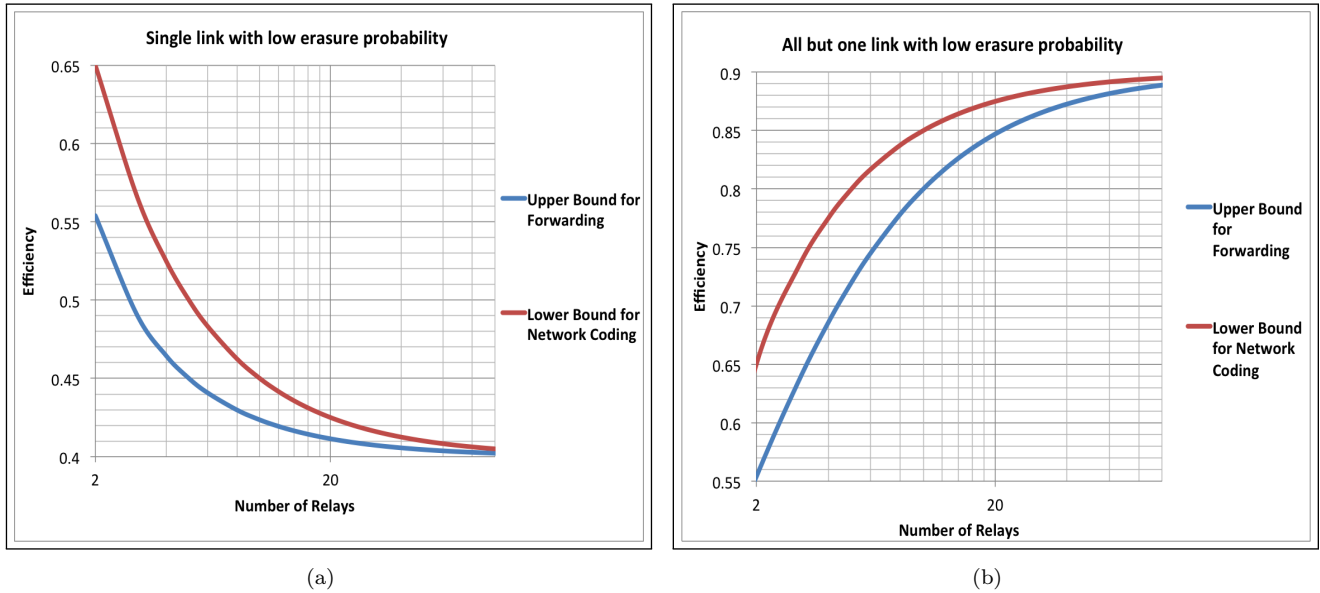


Figure 2: Upper and Lower Bounds for Forwarding and Network Coding respectively for Downlink transmissions: (a) for the case where there is a single link with low packet erasure probability, and (b) for the case where all but one link has low packet erasure probability. Low erasure probability of 0.1 and High erasure probability of 0.6.

Millimeter-wave channel conditions can vary rapidly as shown in [19]. In particular, a link can quickly change among line-of-sight, non-line-of-sight and outage states. Our study implicitly assumes that the channel state is not known with certainty before transmitting a packet to the device. Our intention is to compare performance of the network coding based data transmission via several relay nodes to a transmission approach in which non-network-coded packets are transmitted via several relay nodes. We refer to the latter approach as “Forwarding”. In this section, we first describe Random Linear Network Coding, after which we describe the scheduling mechanisms for the downlink and the uplink communication and provide some performance bounds.

3.1 Random Linear Network Coding

Given a set of k packets $[P_1, P_2, \dots, P_k]$ chosen from a Galois Field alphabet F , a random linear network-coded packet is constructed as $\sum_{i=1}^k c_i \cdot P_i$ where $[c_1, c_2, \dots, c_k]$ is an “encoding vector” consisting of a set of coefficients randomly chosen from F . If a receiver receives k packets $[r_1, r_2, \dots, r_k]$ with encoding vectors $[c_1^i, c_2^i, \dots, c_k^i]$ corresponding to each r_i , it can construct a transfer matrix:

$$M = \begin{pmatrix} c_1^1 & c_2^1 & \dots & c_k^1 \\ c_1^2 & c_2^2 & \dots & c_k^2 \\ \vdots & \vdots & \ddots & \vdots \\ c_1^k & c_2^k & \dots & c_k^k \end{pmatrix}$$

The receiver can then recover the original packets using $M^{-1} \cdot [r_1, r_2, \dots, r_k]^T$. The probability of M not having an inverse can be made sufficiently small by choosing a large F .

3.2 Scheduling and Data Transmission

In this study, time is divided into time-spans, with each time span having multiple time-slots. A time-slot is the time duration of one transmission over the air-interface. A number of packets k are to be delivered in each time-span. In each time span the transmitting side attempts to deliver the k packets to the receiving side through relays. The Forwarding approach and the Network coding approach are described as follows:

- **Forwarding:** For each of the k packets, a relay node is selected. The transmitting side then performs transmissions until the packet is received.
- **Network Coding:** For downlink communication, while the k packets are not decoded, the transmitting side (a) generates a Random Linear Network Coded (RLNC) packet from the k original packets, (b) chooses a relay node, and (c) transmits the RLNC packet through the chosen relay node. For the uplink communication, any relay node that has received a subset of packets forms a network coded packet from the subset and transmits it to the network.

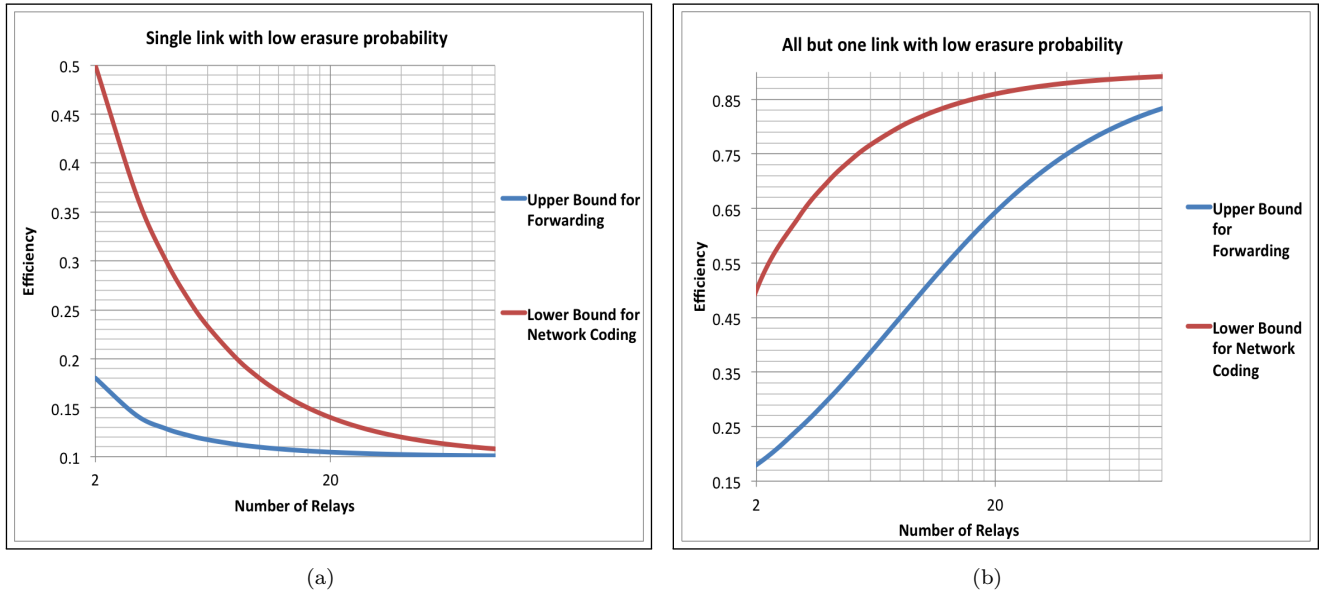


Figure 3: Upper and Lower Bounds for Forwarding and Network Coding respectively for Downlink transmissions: (a) for the case where there is a single link with low packet erasure probability, and (b) for the case where all but one link has low packet erasure probability. Low erasure probability of 0.1 and High erasure probability of 0.9.

We compare the efficiency of the two approaches, which we define as the ratio of the number of packets delivered to the number of transmissions needed to deliver the packets. Estimating other metrics such as throughput and delay requires specific assumptions regarding the physical layer communication (e.g., transmission slot duration, bandwidth, etc.). Although we do not model such specific physical layer parameters, the efficiency metrics used are directly related to throughput and delay. For example, a higher efficiency translates to a higher data rate. A higher efficiency can also translate to lower average packet delivery delay.

Comparing Network Coding to the Forwarding approach as described above is motivated by having an “apples-to-apples” comparison. That is, since the network coding approach uses multiple relay nodes, we compare it to an approach that does not use network coding, but still utilizes multiple relay nodes. Abstracting away from the physical layer details, the Forwarding approach is similar to Coordinated Multi-point Transmission in LTE [20]. In the following we study two types of network coding, namely: *Intra-session network coding* for downlink communication, and *Inter-session network coding* for uplink communication.

3.2.1 Single Device - Intra-session Network Coding for Downlink

We first consider a setup in which the network is

transmitting data to a single device D through N relay nodes. Forwarding and Network Coding are performed as described above and the selection of relays is based on a uniform random distribution. To derive the efficiency of the two approaches, let R_1, R_2, \dots, R_N be the relay nodes, P_1, P_2, \dots, P_k be the packets to be transmitted in the time-span, and p_1, p_2, \dots, p_N be the packet erasure probabilities of the links from the corresponding relay nodes to D .

For the forwarding approach, given the random selection of relay nodes, each relay node is expected to transmit $\lceil \frac{k}{N} \rceil$ original packets on average. The expected value of the number of transmissions through relay node R_i is $\lceil \frac{k}{N} \rceil \frac{1}{(1-p_i)}$. The total number of transmissions to deliver the k packets is $\sum_{i=1}^N \lceil \frac{k}{N} \rceil \frac{1}{(1-p_i)}$. The efficiency for the Forwarding approach is therefore:

$$eff_F = \frac{k}{\lceil \frac{k}{N} \rceil \sum_{i=1}^N \frac{1}{(1-p_i)}} \quad (1)$$

Observing that $\lceil \frac{k}{N} \rceil \geq \frac{k}{N}$, we derive an *upper bound* for the forwarding efficiency:

$$eff_F \leq \frac{N}{\sum_{i=1}^N \frac{1}{(1-p_i)}} \quad (2)$$

For the Network Coding approach, let $\mathcal{P}_1, \mathcal{P}_2, \dots, \mathcal{P}_L$ be the RLNC packets that are transmitted through the relay nodes to deliver the original packets P_1, P_2, \dots, P_k .

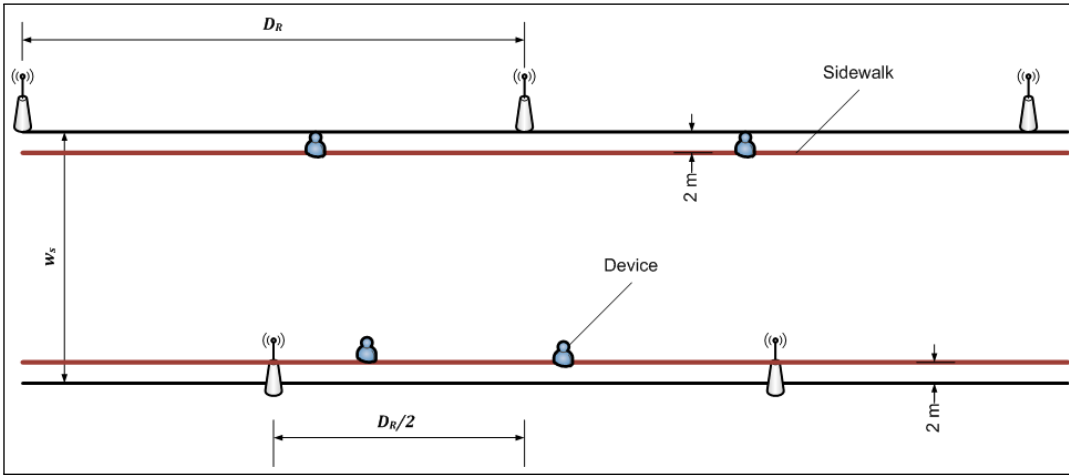


Figure 4: Deployment scenario for simulation: Users are randomly dropped on sidewalks, and relays are equally spaced on each side of the street

Given the random selection of relay nodes, each relay node is expected to transmit $\lceil \frac{L}{N} \rceil$ RLNC packets on average. Of the number of RLNC packets transmitted through a given relay node, the number that is successfully received follows a binomial distribution with parameters $\lceil \frac{L}{N} \rceil$ and p_i . The expected value of the number of RLNC packets received through R_i is $\lceil \frac{L}{N} \rceil (1 - p_i)$. The total number of RLNC packets transmitted to deliver the k original packets is $\sum_{i=1}^N \lceil \frac{L}{N} \rceil (1 - p_i)$. In order to decode the k original packets, k RLNC packets need to be received. Therefore we have:

$$k = \lceil \frac{L}{N} \rceil \sum_{i=1}^N (1 - p_i) \quad (3)$$

The efficiency of the network coding approach is therefore:

$$eff_C = \frac{\lceil \frac{L}{N} \rceil \sum_{i=1}^N (1 - p_i)}{L} \quad (4)$$

Noting that $\lceil \frac{L}{N} \rceil \geq \frac{L}{N}$, we derive the following *lower bound* for network coding:

$$eff_C \geq \frac{\sum_{i=1}^N (1 - p_i)}{N} \quad (5)$$

Note that the difference between the forwarding and the network coding approaches is that for the forwarding case, a single node is responsible for delivering a particular packet leading to bound (2) whereas for the network coding case, it is sufficient to correctly receive a total of k packets that may have been received via multiple nodes.

To understand how the two schemes perform compared to each other, the best (i.e., upper bound) performance of forwarding is compared to the worst (i.e.,

lower bound) performance of network coding for three different scenarios described in the following. In the first scenario, $p_i = p, \forall i$. In this scenario, we get $eff_F \leq 1 - p \leq eff_C$. That is, when all links have equal erasure probability, network coding performs at least as well as forwarding.

Figures 2 and 3 show a comparison of the efficiency bounds for a second and a third specific scenario respectively. For the second scenario, Figure 2a, one link from D to one of the Relays has a low packet erasure probability, while all the other links to the Relays have a high packet erasure probability. For the third scenario, Figure 2b, one link from D to one of the relays has a high packet erasure probability, while all the other links have a low packet erasure probability. For both asymmetric erasure probability cases a low and high packet erasure probabilities of 0.1 and 0.6 respectively are assumed. Similarly, Figure 3 shows a corresponding comparison of the efficiency bounds for asymmetric cases with low and high packet erasure probabilities of 0.1 and 0.9 respectively. That is, Figure 3a shows the upper bound for forwarding efficiency and the lower bound for network coding efficiency with a single link having low erasure probability and all other links having high erasure probability. Figure 3b shows the upper bound for forwarding efficiency and the lower bound for network coding efficiency with a single link having high erasure probability and all other links having low erasure probabilities.

The main observation from Figures 2 and 3 is that the performance improvements that are expected for network coding relative to forwarding are larger for scenarios where there is a larger difference between the era-

sure probabilities on the different links. It is also worth emphasizing that Figure 2 and Figure 3 show upper and lower bounds for the forwarding efficiency and the network coding efficiency, respectively. That is, under the assumptions made above, *forwarding is expected to perform no better than and network coding is expected to perform at least as well as the efficiency plots shown.*

3.2.2 Multiple Devices - Inter-session Network Coding for Uplink

We now consider a setup in which devices $D1, D2, \dots, Dz$ transmit to the network through Relay nodes R_1, R_2, \dots, R_N . The goal is to compare the efficiency of the backhaul usage for forwarding and network coding.

Each device transmits one packet in a time span, with re-transmissions as necessary to ensure that at least one of the relay nodes receives the packet. For the forwarding approach, each Relay node simply transmits to the network the packets that it has received¹. For the network coding approach, each Relay node constructs network-coded packets from the original packets it has received and transmits them to the network over the backhaul link. Specifically, if a relay node does not receive a packet from a particular device, it uses an encoding coefficient of 0 corresponding to that device; otherwise, a non-zero encoding coefficient is randomly chosen. Once an adequate number of packets are received to be able to decode the original packets at the network side in the time span, the relay nodes do not transmit further network-coded packets during that time span.

To calculate the backhaul efficiency, let P_1, P_2, \dots, P_z be the packets from $D1, D2, \dots, Dz$ in a time span. Let $p_{i,1}, p_{i,2}, \dots, p_{i,N}$ be the packet erasure probabilities for the links from Di to R_1, R_2, \dots, R_N . As mentioned above, each device Di transmits its packet P_i until it is received by at least one of the relay nodes. The expected number of transmissions of P_i can be written as:

$$\mathbb{E}[[P_i]] = \frac{1}{1 - \prod_{j=1}^N p_{i,j}}. \quad (6)$$

The probability distribution of the number of times $r_{i,j}$ that P_i is received successfully at R_j from n_i transmissions of P_i , follows a binomial distribution. Thus the probability that P_i is received successfully at R_j at least once is $1 - p_{i,j}^{n_i}$. We approximate the probability of R_j receiving P_i as $1 - (p_{i,j})^{\mathbb{E}[[P_i]]}$. For forwarding, given that the Relays simply transmit the packets received

from the devices, the expected value of the number of backhaul transmissions of P_i is obtained by summing over the relay nodes, i.e., $\sum_{j=1}^N (1 - (p_{i,j})^{\mathbb{E}[[P_i]]})$. The expected value of the number of backhaul transmissions of all packets P_1, P_2, \dots, P_z is given by:

$$\sum_{i=1}^z \sum_{j=1}^N (1 - (p_{i,j})^{\mathbb{E}[[P_i]]}) \quad (7)$$

assuming no acknowledgment feedback from the network to relays for each individual packet. The backhaul efficiency is defined as the ratio of the number of original packets per time span to the average number of backhaul transmissions per time span. The expected value of the backhaul efficiency is approximated as:

$$bkEff_F \approx \frac{z}{\sum_{i=1}^z \sum_{j=1}^N (1 - (p_{i,j})^{\mathbb{E}[[P_i]]})} \quad (8)$$

For erasure probabilities that are close to 1, the approximation of Eq (8) can yield efficiency values that are greater than 1. This is due to the fact that the expected value of the number of backhaul transmissions of P_i , as represented by $\sum_{j=1}^N (1 - (p_{i,j})^{\mathbb{E}[[P_i]]})$, is less than 1 for cases where N is small and $p_{i,j}$ are close to 1. However, since the number of backhaul transmissions of P_i is at least 1 in practice, we modify Eq (8) as follows²:

$$bkEff_F \approx \frac{z}{\sum_{i=1}^z \max(1, \sum_{j=1}^N (1 - (p_{i,j})^{\mathbb{E}[[P_i]]})} \quad (9)$$

For the Network Coding case, the backhaul efficiency calculation involves subtleties in matrix rank calculation considering each relay may have received a subset of packets to be network-coded. In the following, a lower bound on the efficiency is obtained for the scenario in which $\forall i, j, p_{i,j} = p$, and $N \leq z$,³ and the bound derivation for the *asymmetric* erasure probability cases is left as future work. The main steps of the derivations are provided here, while the details are presented in Appendix 7.

1. The average number of the required backhaul transmissions β_{nc} is upper bounded in Eq (10) (hence providing a lower bound for the backhaul efficiency of network coding). The wireless network needs to collect enough (i.e., β_{nc}) network-coded packets to ensure z of them are independent. The encoding coefficients corresponding to each received network-coded packet are randomly drawn from a Galois field of size q according to the distribution

¹For both Forwarding and Network coding, we assume that a given Relay node has no knowledge of which packets have been received by other Relay nodes. Such knowledge would require extensive signaling between the Relay nodes.

²It is remarked that we found the above approximation to be quite tight through numerous Monte-Carlo simulations, particularly for low to medium erasure probabilities.

³The $N > z$ case is discussed at the end of this section.

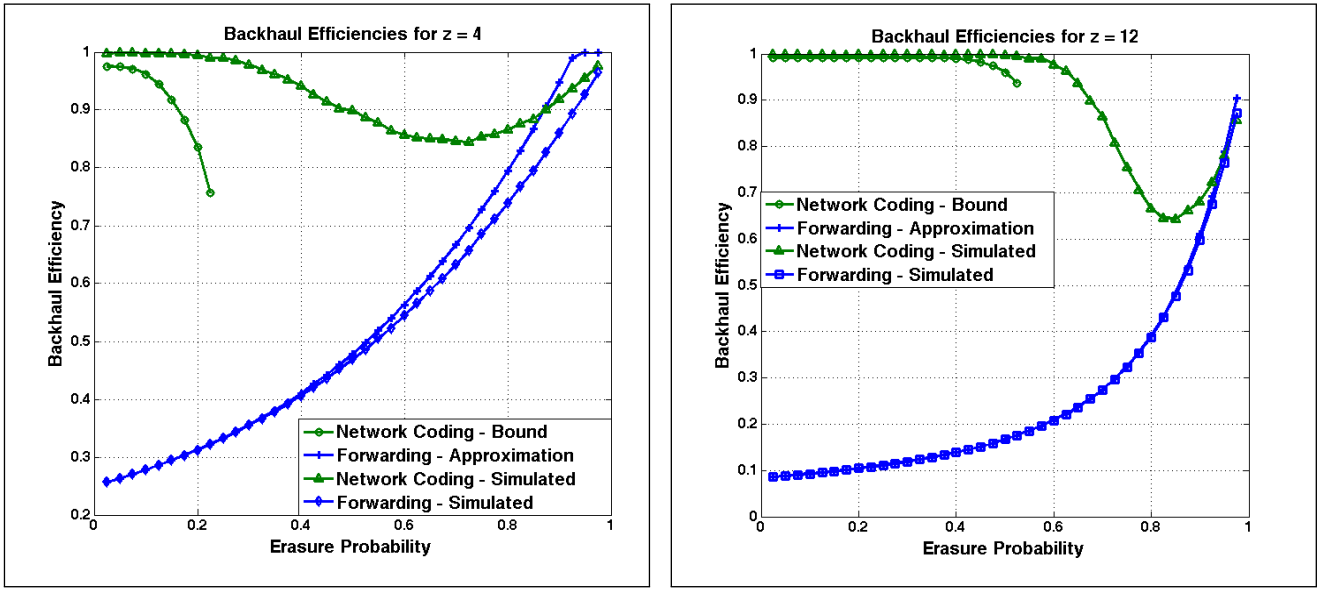


Figure 5: Theoretical and Simulated Backhaul Efficiencies for equal link erasure probabilities

Ω : 0 with probability p , and $w \in \{1, \dots, q-1\}$ with probability $\frac{1-p}{q-1}$. To upper bound β_{nc} , we assume the probability of a randomly chosen $z \times z$ matrix M being singular is ϕ , if each element of the matrix is drawn according to Ω .

$$\beta_{nc}(\phi) \leq \sum_{l=0}^{\infty} (z+l) [1 - \phi^{\zeta(l)-\zeta(l-1)}] \phi^{\zeta(l-1)}, \quad (10)$$

where $\zeta(l) = \binom{z+l}{z}$ and $\zeta(-1) = 0$.

- It is shown that for $\phi \leq \phi_{ub} < 1$, $\beta_{nc}(\phi) < \beta_{nc}(\phi_{ub})$, where

$$\phi_{ub} = \log_q(\bar{l}(M) + 1), \quad (11)$$

and $\bar{l}(M)$ denotes the expected number of linear dependencies of the rows of M (see definition 7.2).

We derive a lower bound for the backhaul efficiency for network coding shown below:

$$bkEff_C \geq \frac{z}{\sum_{l=0}^{\infty} (z+l) [1 - \phi_{ub}^{\zeta(l)-\zeta(l-1)}] \phi_{ub}^{\zeta(l-1)}} \quad (12)$$

The details of the derivation are provided in appendix 7. Note that the bound proposed in Eq (12) is valid for $\phi < 1$, which for a given code length z and field size q , translates to a feasible region for erasure probability p according to Eq. (11).

Since the network coding bound is derived only for the case of symmetric link erasure probability, we compare in this section the backhaul efficiency for both Forwarding and Network Coding assuming $p_{i,j} = p \forall i, j$, and leave the analysis of the general case to Section 4.4.

When $\forall i, j, p_{i,j} = p$:

$$bkEff_F \approx \min \left[1, \frac{1}{N(1 - p^{\frac{1}{1-p^N}})} \right].$$

Figure 5 compares the following: (i) the lower bound of network coding backhaul efficiency, (ii) the approximate forwarding backhaul efficiency, (iii) the simulated backhaul efficiency for network coding, and (iv) the simulated backhaul efficiency for forwarding. Figure 5(a) and Figure 5(b) show the comparison for $z = 4$ and $z = 12$ respectively, and $q = 1024$ is assumed for both. It can be seen from the figure that:

- The network coding backhaul efficiency bound is applicable to a range of erasure probability p , and outside of this range, $bkEff_C$ is undefined. The range of p for which $bkEff_C$ is defined corresponds to $0 \leq \phi < 1$. Additionally, increasing the code length z increases the range over which $bkEff_C$ is defined.
- The network coding efficiency is close to 1 for a range of erasure probabilities. As code length z increases the range of erasure probabilities for which the efficiency is close to 1 grows.
- For medium to high erasure probabilities, the network coding lower bound in Eq (12) deviates significantly from the simulated network coding backhaul efficiency. The following is an explanation for this deviation. Note that Eq (12) does not take into account which relay nodes transmit the packets. Consequently, it includes cases where a relay

node transmits redundant packets to the network (for example, a relay node may transmit a first network coded packet based on an encoding vector $[c_1, 0, 0, 0]$ and a later network coded packet based on an encoding vector $[c_2, 0, 0, 0]$, where c_1 , and c_2 are randomly chosen coefficients from alphabets of the field). In the computation of the simulated network coding backhaul efficiencies, transmission of such redundant packets is avoided. The redundant transmissions cause a gap between the lower bound and the simulated backhaul efficiency, and the size of the gap increases with increasing erasure probabilities. Deriving a tighter lower bound for the network coding backhaul efficiency by avoiding transmission of redundant network coded packets is a topic for further study.

We make a final remark regarding the $N > z$ case. If relay nodes transmit their respective network coded packets at the same time, it is possible that one network coded packet from each relay node (i.e., N network coded packets) is transmitted to the network although fewer than N network coded packets are needed to decode the z packets. In such a case, the upper bound on the number of backhaul transmissions would be $\max(N, \beta_{nc}(\phi_{ub}))$. Thus, if $N > z$ and p is small, there can be redundant transmissions, which in turn reduces the backhaul efficiency for network coding. Consequently, it is not beneficial to use more than z relay nodes in such cases.

4. SIMULATION

4.1 Deployment Scenario

In this section, Monte-Carlo system simulation results are provided to evaluate the benefits of network coding compared to the forwarding approach. It is assumed that N_R relay nodes are placed uniformly spaced on two sides of a street with width w_s . The distance between the relays is D_R , and relay nodes on one side of the street are shifted by $\frac{D_R}{2}$ with respect to the relay nodes on the other side. The street has a sidewalk at 2 meters from each edge. N_{ue} user devices are uniformly randomly dropped on sidewalks. Figure 4 shows the simulation setup.

4.2 Channel Model

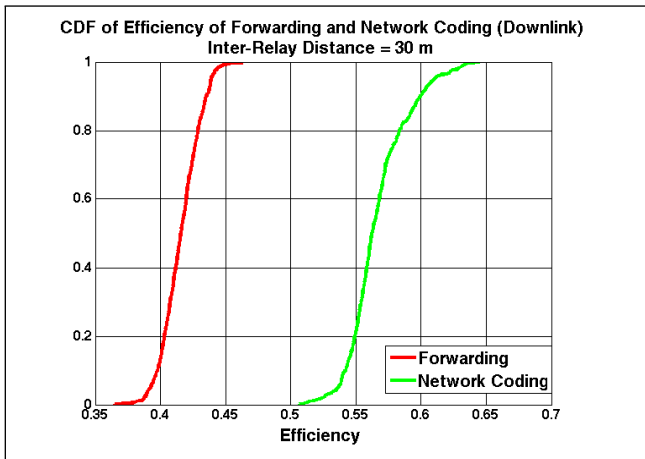
In this work, a packet erasure $p_{i,j}$ is associated with the link between device i and relay node j , and a packet is assumed to be received correctly with probability $1 - p_{i,j}$ at the destination. The channel model illus-

trated in [19] is used to capture fundamental characteristics of the millimeter-wave channels, namely high path-loss, and frequent outage. In particular, a link is assumed to be in Outage, Line-of-Sight or Non-Line-of-Sight states with certain device-relay node distance based probabilities, as described in [19]. If a link is in outage, the corresponding packet erasure probability is 1. If the link is in line-of-sight or non-line-of-sight states, the link erasure probability is set to the block error rate (BLER) corresponding to that link. To obtain the BLER, path-loss is computed according to the path-loss model for 28 GHz described in [19]. Then SNR is derived based on assumed parameter values for beamforming gain, transmit-power, coding gain, as well as path-loss. Once SNR is calculated, BLER is determined assuming 64 QAM transmissions for the downlink and QPSK transmissions for the uplink, respectively. Further, if the erasure probability of a link is higher than a threshold T_e , that link is not used for communication and is assumed to be in outage. The parameter values used and other details are listed in appendix 8.

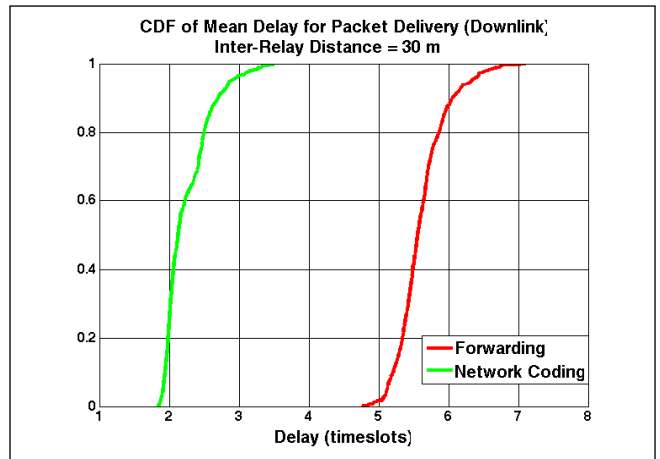
4.3 Downlink Simulations

In this section, we discuss simulation results comparing the Forwarding and Network Coding approaches for downlink transmissions to the devices (i.e., intra-session network coding as described in section 3.2.1). For this simulation, 5000 devices are randomly dropped across the deployment detailed in section 4.1. During each time span, we compare efficiency and packet delay metrics for transmissions of k packets using the forwarding approach and the network coding approach, as described in section 3.2. Figure 6a, Figure 6c and Figure 6e show the CDF of efficiency calculated for each device for Forwarding and Network Coding approaches for D_R of 30 meters, 60 meters and 80 meters, respectively. The gain of network coding compared to forwarding increases with increasing density of relay nodes. For example, the case with $D_R = 30$ meters shows a larger gain for network coding compared to that of $D_R = 60$ meters and $D_R = 80$ meters. This behavior is attributed to having more outage-free links at higher relay node densities (although the links have varying error rates). The improvement in efficiency points to an increase in data rates of 35%-39% for network coding compared to forwarding, for D_R of 30 meters. The case with D_R of 60 meters shows an increase in data rates of 11%-37%. The case with D_R of 80 meters shows an increase in the range of 3%-34%.

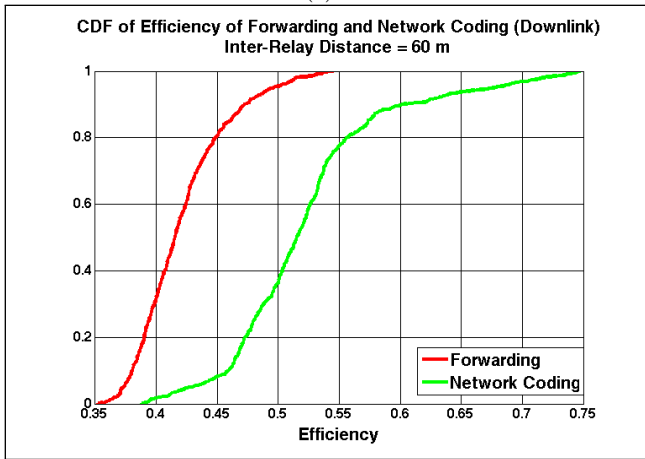
Figure 6b, Figure 6d and Figure 6f show the delay in



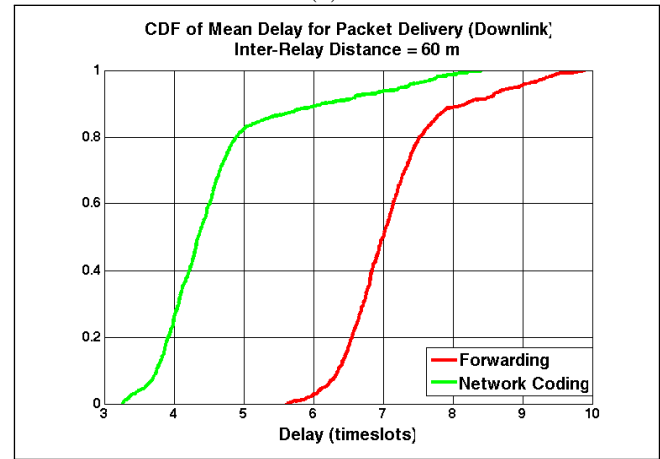
(a)



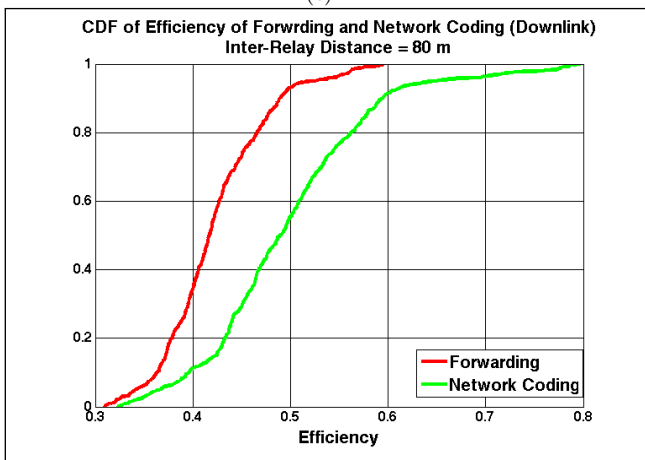
(b)



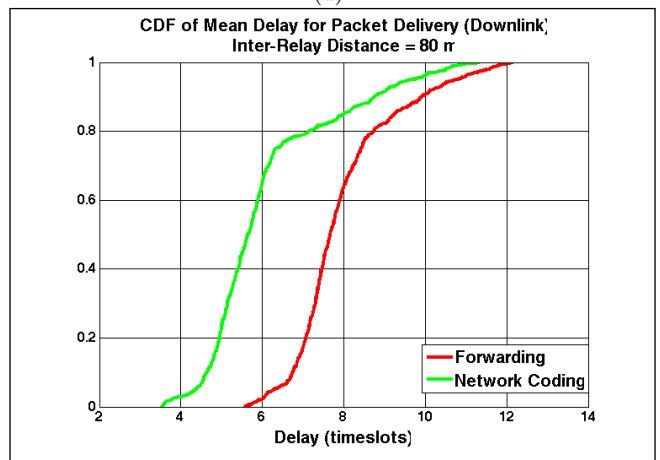
(c)



(d)

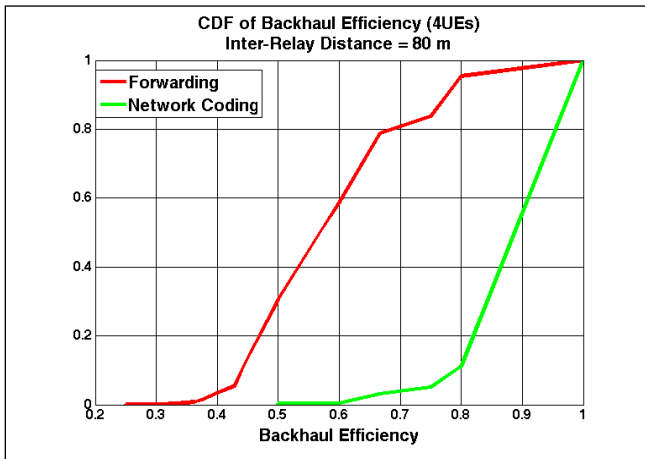


(e)

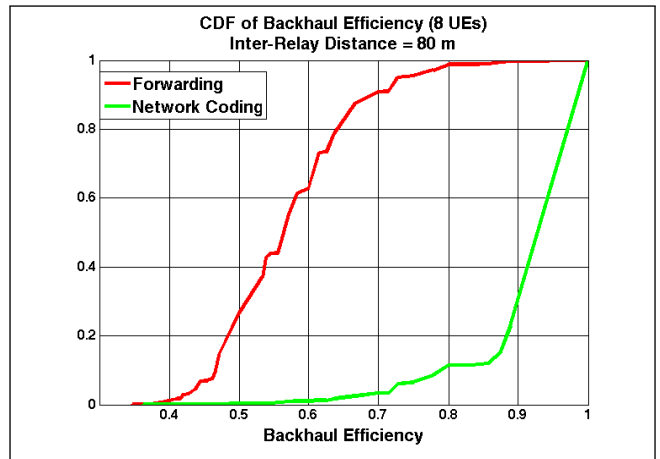


(f)

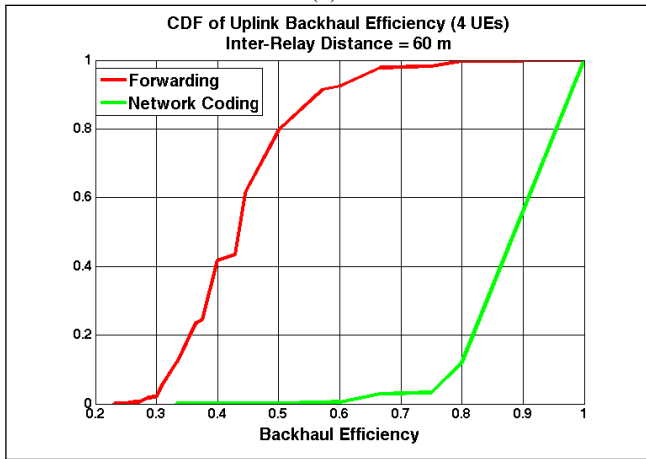
Figure 6: Downlink efficiency and delay performance of network coding compared to forwarding for different relay densities



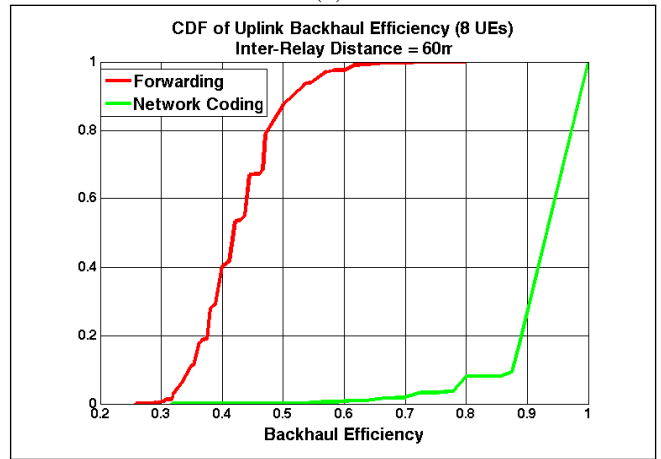
(a)



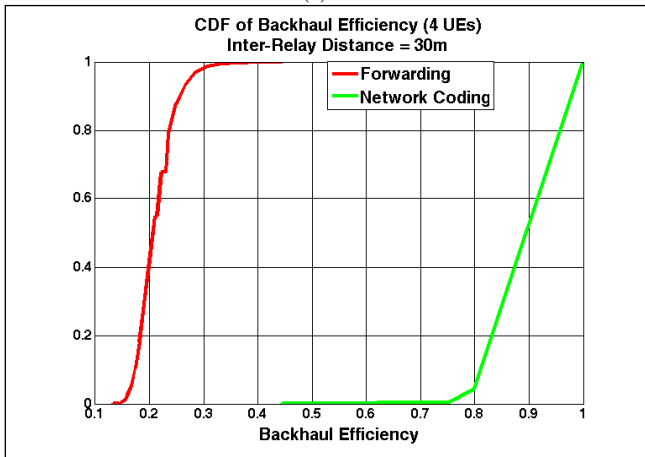
(b)



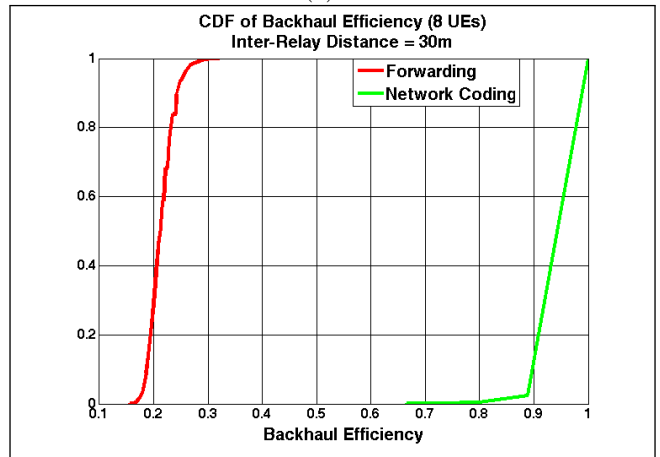
(c)



(d)



(e)



(f)

Figure 7: Uplink backhaul efficiency network coding compared to forwarding for different network code length (number of devices) and relay densities

delivering the packets in each time-span. As mentioned previously, k packets are delivered in each time-span. The delay represents the number of time-slots used for transmissions (i.e., transmission time) until all the k packets are received at the device. As shown, network coding yields significant reductions in the delays. The gains are more significant for D_R of 30 meters, i.e., the denser deployment, and decrease with decreasing relay node density.

4.4 Simulation of Backhaul Efficiency in Uplink

In this section, we discuss simulation results comparing the Forwarding and Network Coding approaches for uplink transmissions (i.e., inter-session network coding as described in section 3.2.2) with $k = 1$ to capture the multi-user nature of the uplink problem. Figure 7a and Figure 7b show a comparison of the backhaul efficiencies for the Forwarding and the Network Coding approaches, when packets of 4 and 8 devices are combined at relay nodes respectively, for $D_R = 80$ meters. Figure 7c and Figure 7d, and Figure 7e and Figure 7f show corresponding comparisons of the backhaul efficiencies for $D_R = 60$ meters and $D_R = 30$ meters, respectively. As can be seen from Figure 7, the backhaul efficiency of network coding improves relative to forwarding when either (a) the inter-relay distance is reduced, or (b) the number of devices is increased. The median network coding backhaul efficiency with 4 devices is approximately 57%, 100% and 320% better than the median forwarding backhaul efficiency for inter-relay distances of 80, 60 and 30 meters, respectively. With 8 devices, the median network coding backhaul efficiency is approximately 63%, 123% and 352% better than the median forwarding backhaul efficiency for inter-relay distance of 80, 60 and 30 meters, respectively. The improvement in backhaul efficiencies directly translate to reduction in backhaul traffic - for example, the 100% improvement in backhaul efficiency due to network coding with 4 devices for the $D_R = 60$ meter case corresponds to a 50% reduction in backhaul traffic.

5. CONCLUSION

We have analyzed and quantified the benefits of Random Linear Network Coding in millimeter-wave communication systems with a dense deployment of access points, where individual links show a lot of variation. For our analysis and comparisons, we use the ratio of number of packets delivered to the number of transmissions needed for delivery of the packets as an efficiency

metric. For downlink communication, we focus on the efficiency of network coding for the air-interface transmissions, whereas for uplink communication, we focus on the efficiency of network coding for the backhaul transmissions.

We have provided a theoretical upper bound for the expected values of efficiency of downlink air-interface transmissions for Forwarding and a theoretical lower bound for the expected values of efficiency for Network Coding. For the scenarios of interest, we observe that the lower bound for the expected value of efficiency of network coding is higher than the upper bound of the expected value of efficiency for forwarding. This implies that network coding is expected to outperform forwarding, with the difference being dependent on the diversity of packet erasure probabilities for the links.

We have derived a lower bound on the uplink backhaul efficiency of the network coding for the case of user-to-relay links with equal packet erasure probability. The bound is applicable to a range of erasure probabilities (low to medium) and implies that network coding can maintain a backhaul efficiency of close to 1 even for small network code lengths. The range of erasure probabilities for which the bound is applicable increases with increasing network code lengths. We also provided a tight approximation for the backhaul efficiency for the forwarding case. Comparing the lower bound of network coding to the approximate backhaul efficiency of forwarding, we have shown that network coding offers not only a much higher efficiency (multiple times better) but also a universal backhaul efficiency close to one for the applicable region of erasure probabilities.

For the simulation, we use a millimeter wave channel model along with probabilities of links being in outage, non-line-of sight or line-of-sight, to capture the rapidly changing nature of the individual links. For the downlink intra-session network coding, our results show a significant improvement in the efficiency of air-interface transmissions with the use of network coding. The extent of improvement depends on the density of the Relay nodes (as represented by the parameter D_R). For example, with Relay nodes deployed every 30 m on each side of the street, we see a median improvement of 35% in efficiency, which in turn translates to correspondingly higher data rates and shorter transmission durations.

For the uplink inter-session network coding, our results show a significant improvement in the efficiency of backhaul transmissions with the use of network coding. For example, with Relay nodes every 60 m on each side of the street, we see a median improvement in backhaul

efficiency of 100% with 4 devices and 123% with 8 devices (i.e. 50% and 55% lower backhaul traffic for the same number of packets respectively).

It is remarked that this study aimed to characterize fundamental benefits of network coding in 5G wireless networks. To achieve this goal a few assumptions about the physical layer transmission procedures and protocols are made to simplify the system model. Therefore, our observations and comparison metrics are useful only in a relative sense. In order to understand the performance of network coding in more absolute terms (e.g., spectral efficiency improvement in b/s/Hz or latency reduction in milliseconds) it is necessary to have a more comprehensive study using a detailed physical layer channel structure. The details of such channel models will be discussed in the coming months in standards bodies such as 3GPP.

6. REFERENCES

- [1] “Cisco Visual Network Index: Global Mobile Traffic Forecast 2014-2019”, 2015.
- [2] “Mobile traffic forecasts: 2010-2020 report,” in UMTS Forum Report, vol. 44, 2011.
- [3] A. Osseiran, F. Boccardi, V. Braun, K. Kusume, P. Marsch, M. Maternia, O. Queseth, M. Schellmann, H. Schotten, H. Taoka et al., “Scenarios for 5G mobile and wireless communications: the vision of the METIS project,” *IEEE Commun. Mag.*, vol. 52, no. 5, pp. 26–35, May 2014.
- [4] F. Boccardi, R. Heath, A. Lozano, T. L. Marzetta, and P. Popovski, “Five disruptive technology directions for 5G”, *IEEE Commun. Mag.*, vol. 52, no. 2, pp. 74–80, Feb. 2014.
- [5] J. G. Andrews, S. Buzzi, W. Choi, S. Hanly, A. Lozano, A. C. Soong, and J. C. Zhang, “What will 5G be?”, *IEEE J. Select. Areas Commun.*, vol. 32, no. 6, pp. 1065–1082, Jun. 2014.
- [6] Z. Pi and F. Khan, “An Introduction to Millimeter-Wave Mobile Broadband Systems”, *IEEE Commun. Mag.*, vol 49, no 6, pp.101–107, Jun 2011.
- [7] S. Rangan, T. Rappaport, and E. Erkip, “Millimeter wave cellular wireless networks: Potentials and challenges,” *Proc. IEEE*, vol. 102, no. 3, pp. 366–385, Mar. 2014.
- [8] T. S. Rappaport, R. Heath, R. C. Daniels, and J. N. Murdock, *Millimeter Wave Wireless Communications*. Pearson Education, 2014.
- [9] T. S. Rappaport, J. N. Murdock, and F. Gutierrez, “State of the art in 60-GHz integrated circuits and systems for wireless communications,” *Proc. IEEE*, vol. 99, no. 8, pp. 1390–1436, Aug. 2011.
- [10] “Millimeter-wave communications for 5G: Fundamental: Part I,” *IEEE Commun. Mag.*, special issue on, vol. 52, no. 9, Sept. 2014.
- [11] H. Shokri-Ghadikolaei, C. Fischione, G. Fodor, P. Popovski, and M. Zorzi, “Millimeter Wave Cellular Networks: A MAC Layer Perspective,” newblock *IEEE Transactions on Communications*, July 2015, accepted for publication.
- [12] A. Talukdar, M. Cudak, and A. Ghosh, “Handoff rates for millimeterwave 5G systems,” *IEEE Vehicular Technology Conference (VTC Spring)*, May 2014.
- [13] 3rd Generation Partnership Project, “Evolved Universal Terrestrial Radio Access (E-UTRA) and Evolved Universal Terrestrial Radio Access Network (E-UTRAN); Overall description; Stage 2 (Release 12)”, 3GPP TS 36.300 V12.6.0. <http://www.3gpp.org/DynaReport/36300.htm>.
- [14] R. Ahlswede, N. Cai, S.-Y.R. Li, and R. W. Yeung, “Network information flow,” *IEEE Trans. Inf. Theory*, vol. 46, pp. 1204-1216, 2000.
- [15] Y. Chen, S. Kishore, and J. Li, “Wireless diversity through network coding,” *Proc. IEEE Wireless Commun. and Networking Conf. (WCNC)*, Las Vegas, USA, Apr. 2006.
- [16] X. Bao and J. Li, “Matching code-on-graph with network-on-graph: Adaptive network coding for wireless relay networks,” *Proc. Allerton Conf. on Commun., Control and Computing*, Monticello, USA, Sep. 2005.
- [17] C. Hausl and P. Dupraz, “Joint network-channel coding for the multiple- access relay channel,” *Proc. IEEE Int. Conf. on Sensor, Mesh and Ad Hoc Commun. and Networks (SECON)*, Reston, USA, Sep. 2006.
- [18] J. Blomer, R. Karp, and E. Welzl, “The Rank of Sparse Random Matrices over Finite Fields,” *Random Structures and Algorithms* 10(4), 1997.
- [19] M. R. Akdeniz, Y. Liu, M. K. Samimi, S. Sun, S. Rangan, and T. S. Rappaport, “Millimeter Wave Channel Modeling and Cellular Capacity Evaluation”, *IEEE Journal on Selected Areas of Communications*, Vol 32, No. 6, June 2014.
- [20] D. Lee, H Seo, B Clerckx, E. Hardouin, D. Mazzaresse, S. Nagata and K Sayana, “Coordinated Multipoint Transmission and

7. APPENDIX - BACKHAUL EFFICIENCY DERIVATION FOR NETWORK CODING

In this appendix, the average number of required Backhaul Transmissions (BHT) for network coding, β_{nc} , is obtained. The averaging is done over source-relay link conditions when each source-relay link erasure probability is p . Each backhaul transmission from a relay is a network-coded packet constructed at the relay from z encoding coefficients. The z encoding coefficients are independently and identically distributed elements each drawn according to distribution Ω (see section 3.2.2). The network has to collect z independent network coded packets from the relays in order to decode all the z original packets transmitted from the sources.

Assume that the network has received $z + l$ ($l \geq 0$) BHTs from the relays. If it can construct a full rank $z \times z$ matrix from the set of $z+l$ rows (each row corresponding to the encoding coefficient vector for a network coded packet), the network can decode all the original packets. We use \mathbb{M}_l to denote the set of $\zeta(l) = \binom{z+l}{z}$ possible $z \times z$ matrices that can be constructed from the $z + l$ rows. Each matrix belonging to the set is singular with probability ϕ which is a function of z , p , and the field size q .

The number of required BHT is at most $z + l$ when every matrix M^o in the set \mathbb{M}_{l-1} is singular and there is at least one $z \times z$ matrix M^* in the set \mathbb{M}_l which is non-singular. In the following, the rank of a matrix M is represented by $\nu(M)$, and $Pr(\cdot)$ denotes the probability

of an event.

$$\begin{aligned}
\beta_{nc}(\phi) &= \sum_{l=0}^{\infty} (z+l) Pr(z+l \text{ BHTs are needed}) \\
&\leq \sum_{l=0}^{\infty} (z+l) Pr\left(\exists M^* \in \mathbb{M}_l \setminus \mathbb{M}_{l-1}, \right. \\
&\quad \left. \nu(M^*) = z, \nexists M^o \in \mathbb{M}_{l-1}, \nu(M^o) = z\right) \\
&= \sum_{l=0}^{\infty} (z+l) Pr\left(\exists M^* \in \mathbb{M}_l \setminus \mathbb{M}_{l-1}, \nu(M^*) = z \mid \right. \\
&\quad \left. \nexists M^o \in \mathbb{M}_{l-1}, \nu(M^o) = z\right) \\
&\quad \times Pr\left(\nexists M^o \in \mathbb{M}_{l-1}, \nu(M^o) = z\right) \\
&= \sum_{l=0}^{\infty} (z+l) Pr\left(\nexists M^o \in \mathbb{M}_{l-1}, \nu(M^o) = z\right) \\
&\quad \times \left[1 - Pr\left(\nexists M^* \in \mathbb{M}_l \setminus \mathbb{M}_{l-1}, \right. \right. \\
&\quad \left. \left. \nu(M^*) = z \mid \nexists M^o \in \mathbb{M}_{l-1}, \nu(M^o) = z\right)\right] \\
&= \sum_{l=0}^{\infty} (z+l) \phi^{\zeta(l-1)} [1 - \phi^{\zeta(l) - \zeta(l-1)}] \quad (13)
\end{aligned}$$

The following lemma proves that for $\phi \leq \phi_{ub}$, we have $\beta_{nc}(\phi) \leq \beta_{nc}(\phi_{ub})$.

LEMMA 7.1. $\beta_{nc}(\phi)$ is a non-decreasing function of ϕ .

PROOF. In the following, it is shown that $\frac{d\beta_{nc}}{d\phi} > 0$ for $0 < \phi < 1$.

$$\begin{aligned}
\frac{d\beta_{nc}}{d\phi} &= \frac{d}{d\phi} \left[\sum_{l=0}^{\infty} (z+l) [1 - \phi^{\zeta(l) - \zeta(l-1)}] \phi^{\zeta(l-1)} \right] \\
&= \frac{d}{d\phi} \left[\sum_{l=0}^{\infty} (z+l) (\phi^{\zeta(l-1)} - \phi^{\zeta(l)}) \right] \\
&= \frac{d}{d\phi} \left[z(1 - \phi) + \sum_{l=1}^{\infty} (z+l) (\phi^{\zeta(l-1)} - \phi^{\zeta(l)}) \right] \\
&= -z + \sum_{l=1}^{\infty} (z+l) \zeta(l-1) \phi^{\zeta(l-1)-1} \\
&\quad - \sum_{l=1}^{\infty} (z+l) \zeta(l) \phi^{\zeta(l)-1} \\
&= -z + \sum_{l=0}^{\infty} (z+l+1) \zeta(l) \phi^{\zeta(l)-1} \\
&\quad - \sum_{l=1}^{\infty} (z+l) \zeta(l) \phi^{\zeta(l)-1} \\
&= -z + (z+1) \zeta(0) \phi^{\zeta(0)-1} + \\
&\quad \sum_{l=1}^{\infty} (z+l+1) \zeta(l) \phi^{\zeta(l)-1} - \sum_{l=1}^{\infty} (z+l) \zeta(l) \phi^{\zeta(l)-1} \\
&= \sum_{l=0}^{\infty} \zeta(l) \phi^{\zeta(l)-1} > 0.
\end{aligned}$$

□

Next we derive an upper bound ϕ_{ub} for the probability ϕ of a $z \times z$ matrix with elements drawn according to distribution Ω . $d(M)$ is used to denote $z - \text{rank}(M)$, called the *defect* of M . First we restate the following results from [18].

DEFINITION 7.2. *Let M be a $z \times z$ matrix over Galois field $GF[q]$. Let M_1, \dots, M_z denote the rows of M . A vector $(c_1, \dots, c_z) \in (GF[q])^z$ such that not all c_i are zero is called a linear dependency of M_1, \dots, M_z iff $\sum_{i=1}^z c_i M_i = 0$.*

THEOREM 7.3. *(Lemma 3.2 and Theorem 3.3 of [18]) Let M be a random $z \times z$ matrix over a Galois field of size q , where elements of M are chosen according to the probability distribution Ω . Let $d(M)$ denote the defect of M and $l(M)$ denote the number of linear dependencies of the rows of M . Then,*

$$q^{d(M)} - 1 = l(M). \quad (14)$$

The expected number of linear dependencies of the rows of M is:

$$\bar{l}(M) = \sum_{k=1}^z \binom{z}{k} \frac{1}{q^{z-k}} \left(1 - \frac{1}{q}\right)^k \left[1 + (q-1) \left(1 - \frac{q(1-p)}{q-1}\right)^k\right]^z. \quad (15)$$

Now we show that

LEMMA 7.4. $\phi \leq \phi_{ub}$ where $\phi_{ub} \triangleq \log_q(\bar{l}(M) + 1)$.

PROOF. Let ν denote the rank of the random $z \times z$ matrix M . Let $d(M)$ denote the defect of matrix M (i.e., $z - \nu$) and $\bar{d}(M)$ denote the expected value of the defect of M . It is first shown that for the random matrix M , $\phi \leq \bar{d}(M)$, and then $\bar{d}(M) \leq \phi_{ub}$.

$$\begin{aligned} \bar{\nu} &= \sum_{k=1}^z k Pr(\nu = k) \\ &= \sum_{k=1}^{z-1} k Pr(\nu = k) + z(1 - \phi) \\ &\leq (z-1) \sum_{k=1}^{z-1} Pr(\nu = k) + z(1 - \phi) \\ &= (z-1)\phi + z(1 - \phi) \\ \bar{\nu} &\leq z - \phi \end{aligned} \quad (16)$$

From Eq (16), given that $\bar{d}(M) = z - \bar{\nu}$, we have $\phi \leq \bar{d}(M)$. From Eq (14) we have $d(M) = \log_q(l(M) + 1)$. Therefore, $\bar{d}(M) = \mathbb{E}[\log_q(l(M) + 1)]$. Using the concavity property of the logarithm function, we have

$$\bar{d}(M) \leq \log_q(\bar{l}(M) + 1). \quad (17)$$

□

Based on Lemmas 7.1, and Eq (13) we have:

$$\beta_{nc}(\phi) \leq \beta_{nc}(\phi_{ub}).$$

Substituting ϕ_{ub} from Lemma 7.4, we have:

$$\beta_{nc}(\phi) \leq \sum_{l=0}^{\infty} (z+l) \times [1 - \phi_{ub}^{\zeta(l) - \zeta(l-1)}] \times \phi_{ub}^{\zeta(l-1)}.$$

8. APPENDIX - SIMULATION PARAMETERS

| Parameters | Values |
|---|---|
| N_R (number of Relay Nodes) | 10 |
| D_R (Inter-relay distance) | 30, 60 and 80 meters |
| w_s (Street Width) | 20 meters |
| Path-loss | Cf. first row of table I[19], 28 GHz parameters |
| Outage, Line of Sight and Non-line of Sight probabilities | Cf. second row of table I and Eq (8)[19] |
| Transmit Power | 30 dBm (Downlink) and 20 dBm (Uplink) |
| Beam-forming Gain | 20 dB (Downlink) and 0 dB (Uplink) |
| Coding Gain | 6 dB |
| Noise Power | -87 dBm |
| Noise Figure | 5 dB |
| Modulation | 64 QAM (Downlink) and QPSK (Uplink) |
| BLER formula | $(1 - p_b)^{\text{block-length}}$, where $p_{b,64QAM} = 0.2917 \text{erfc}(\sqrt{\frac{9SNR}{63}})$, and $p_{b,QPSK} = 0.5 \text{erfc}(\sqrt{SNR})$ |
| block-length | 10000 bits |
| T_e | 0.9 |